

# Half Dyon in SU(2) Yang-Mills-Higgs Theory

G.Q. Wong, K.M. Wong, Z. Dan

*School of Physics*

*Universiti Sains Malaysia, 11800 USM Penang, Malaysia*

## Abstract

We present axially symmetric dyon solutions of half-integer topological charge in SU(2) Yang-Mills-Higgs theory. We construct these solutions with varying  $\phi$ -winding number  $n$  and electric charge parameter  $\eta$  at Higgs self-coupling constant,  $\beta = 0.7782$ . We calculate and investigate its total energy, magnetic charge and electric charge. These half dyon solutions possess finite energy and lie along the negative  $z$ -axis.

# 1 Introduction

In Maxwell theory, a monopole is accompanied by a Dirac string, and the Dirac monopole [1] possessing infinite energy obeys the quantization condition  $2Me/\hbar c = N$ , where  $M$  is the magnetic charge and  $e$  is the U(1) gauge field coupling constant. However, in the presence of a Higgs field in the adjoint representation, the 't Hooft-Polyakov monopole [2] arises in the non-Abelian SU(2) Yang-Mills field, and the Dirac string disappears, resulting in a finite energy monopole with magnetic charge one that is radially symmetrical. The quantization condition in the SU(2) Yang-Mills-Higgs field theory in 3 + 1 dimensions becomes  $Mg/\hbar c = N$ , where  $g$  is the SU(2) gauge field coupling constant.

In 3 + 1 dimensions, the SU(2) Yang-Mills-Higgs (YMH) field theory with the Higgs field in the adjoint representation possesses magnetic monopole configurations, as shown in [2–5]. Among these, the 't Hooft-Polyakov monopole solution is invariant under a U(1) subgroup of the local SU(2) gauge group, has non-zero Higgs mass and self-interaction, and has been found to be spherically symmetric and possess finite energy [2]. However, numerical solutions for monopole configurations with magnetic charges greater than unity cannot possess spherical symmetry, as demonstrated in [5,6]. Exact monopole solutions exist only in the Bogomol'nyi-Prasad-Sommerfield (BPS) limit [4,5], and only numerical solutions have been found when the Higgs field potential is non-vanishing. Other exact solutions include the A-M-A and vortex ring solutions, as well as various mirror symmetric monopole configurations [7], and numerical BPS monopole solutions with no rotational symmetry have also been discussed [8]. Further numerical finite energy monopole solutions include the MAP (monopole-antimonopole-pair), MAC (monopole-antimonopole-chain), and vortex ring solutions [9].

While most of the literature on monopole solutions focuses on those with integer topological magnetic charge, there have been some discussions on half monopoles in recent years. Harikumar et al. [10] demonstrated the existence of generic smooth Yang-Mills (YM) potentials of one-half monopoles, but no exact or numerical solutions were provided. Exact one-half monopole axially symmetric solutions and one-half monopole mirror symmetric solutions with Dirac-like strings were discussed in Ref. [8], but these solutions possess infinite total energy.

Teh et al. [11] recently found a finite energy one-half monopole solution. The 't Hooft magnetic fields of these solutions at spatial infinity correspond to the magnetic field of a positive one-half magnetic monopole located at the origin ( $r = 0$ ) and a semi-infinite Dirac string located on one half of the  $z$ -axis carrying magnetic flux,  $2\pi/g$ , going into the center of the sphere at infinity. Thus, the net magnetic charge of the configuration is zero. The non-Abelian solutions have gauge potentials that are singular along one-half of the  $z$ -axis, while being regular elsewhere. The total energy of this one-half magnetic monopole solution is found to increase with  $\lambda$ .

Dyon refers to a particle possessing both magnetic and electric charges. A dyon with a fixed magnetic charge can possess varying electric charges [12] at the classical level. The dyon solutions of Julia and Zee [13] are time-independent solutions with non-vanishing kinetic energy. However, they are non-self-dual even in the Bogomol'nyi-Prasad-Sommerfield (BPS) limit when the electric charge is non-vanishing. Outside the BPS limit, when  $\lambda$  is non-vanishing, the Julia-Zee solutions are non-self-dual. The exact dyon solutions found by Prasad and Sommerfield [4] are, in fact, Julia and Zee dyon solutions in the BPS limit. These solutions are stable as they represent the absolute minima of the energy [14].

In the paper, we construct the axially symmetric half dyon solutions in YMH theory by extending the works by Teh et al. [11]. We consider the case with  $\phi$ -winding number,  $n \geq 1$  with electric

charge parameter,  $0 \leq \eta < 1$  and the Higgs self-coupling constant,  $\beta$  will be fixed at 0.7782. We also calculate the total energy, net magnetic charge, magnetic dipole moment and total electric charge of the half dyon configurations. The half dyon solutions possess finite energy.

In the next section, we provide a brief overview of the SU(2) Yang-Mills-Higgs field theory. Section 3 outlines the construction of the half dyon solution, including the magnetic ansatz utilized and some of its fundamental characteristics. In section 4, we present and discuss the numerical results of our calculations of the half dyon solution. Finally, we conclude with some comments in section 5.

## 2 The SU(2) Yang-Mills-Higgs Theory

The SU(2) Yang-Mills-Higgs Lagrangian in 3 + 1 dimensions is given by

$$\mathcal{L} = -\frac{1}{4}F_{\mu\nu}^a F^{a\mu\nu} - \frac{1}{2}D^\mu\Phi^a D_\mu\Phi^a - \frac{1}{4}\lambda(\Phi^a\Phi^a - \nu^2)^2 \quad (2.1)$$

with the covariant derivatives of the gauge field strength tensor and Higgs field, respectively

$$\begin{aligned} F_{\mu\nu}^a &= \partial_\mu A_\nu^a - \partial_\nu A_\mu^a + g\epsilon^{abc}A_\mu^b A_\nu^c \\ D_\mu\Phi^a &= \partial_\mu\Phi^a + g\epsilon^{abc}A_\mu^b\Phi^c \end{aligned} \quad (2.2)$$

Here  $g$  is the coupling constant of gauge field. The vacuum expectation value of the Higgs field is  $\nu = \mu/\sqrt{\lambda}$  where  $\mu$  is the Higgs field mass and  $\lambda$  is the Higgs self-coupling constant. Greek indices refer to Minkowski spacetime and takes values  $\mu, \nu = 0, 1, 2, 3$  whereas Latin indices refer to the internal isospin and takes values  $a, b, c = 1, 2, 3$ . The metric used is  $-g_{00} = g_{11} = g_{22} = g_{33} = +1$ . The equations of motion are

$$\begin{aligned} D^\mu F_{\mu\nu}^a &= \partial^\mu F_{\mu\nu}^a + g\epsilon^{abc}A^{b\mu}F_{\mu\nu}^c = g\epsilon^{abc}\Phi^b D_\nu\Phi^c \\ D^\mu D_\mu\Phi^a &= \lambda\Phi^a(\Phi^b\Phi^b - \nu^2) \end{aligned} \quad (2.3)$$

As the parameters  $\mu$  and  $\lambda$  approach zero, the Higgs potential approaches zero as well, and it becomes possible to obtain self-dual solutions by solving the first-order partial differential Bogomol'nyi equation,

$$B_i^a \pm D_i\Phi^a = 0, \quad \text{where } B_i^a = -\frac{1}{2}\epsilon_{ijk}F_{jk}^a \quad (2.4)$$

The electromagnetic field tensor proposed by 't Hooft [2] upon symmetry breaking is

$$\begin{aligned} F_{\mu\nu} &= \hat{\Phi}^a F_{\mu\nu}^a - \frac{1}{g}\epsilon^{abc}\hat{\Phi}^a D_\mu\hat{\Phi}^b D_\nu\hat{\Phi}^c \\ &= \partial_\mu A_\nu - \partial_\nu A_\mu - \frac{1}{g}\epsilon^{abc}\hat{\Phi}^a \partial_\mu\hat{\Phi}^b \partial_\nu\hat{\Phi}^c \end{aligned} \quad (2.5)$$

where  $A_\mu = \hat{\Phi}^a A_\mu^a$ ,  $\hat{\Phi}^a = \Phi^a/|\Phi|$ , and  $|\Phi| = \sqrt{\Phi^a\Phi^a}$ . We can view the 't Hooft electromagnetic field tensor to be composed of both the gauge part  $G_{\mu\nu}$  and the Higgs part  $H_{\mu\nu}$  of the electromagnetic field tensor

$$G_{\mu\nu} = \partial_\mu A_\nu - \partial_\nu A_\mu, \quad H_{\mu\nu} = -\frac{1}{g}\epsilon^{abc}\hat{\Phi}^a \partial_\mu\hat{\Phi}^b \partial_\nu\hat{\Phi}^c$$

subsequently we can define the magnetic field in a similar fashion

$$B_i = -\frac{1}{2}\epsilon_{ijk}F_{jk} = B_i^G + B_i^H \quad (2.6)$$

where  $B_i^G$  and  $B_i^H$  are the gauge part and Higgs part of the magnetic field respectively. The net magnetic charge of the system is

$$M = \int \partial^i B_i d^3x = \oint d^2\sigma_i B_i \quad (2.7)$$

### 3 The Axially Symmetric Half Dyon

#### 3.1 Ansatz

We consider the following time independent axially symmetric magnetic ansatz that leads to the half dyon solutions

$$\begin{aligned} gA_i^a &= -\frac{1}{r}\psi_1(r, \theta)\hat{\phi}^a\hat{\theta}_i + \frac{n}{r\sin\theta}P_1(r, \theta)\hat{\theta}^a\hat{\phi}_i + \frac{1}{r}R_1(r, \theta)\hat{\phi}^a\hat{r}_i - \frac{n}{r\sin\theta}P_2(r, \theta)\hat{r}^a\hat{\phi}_i \\ gA_0^a &= \tau_1(r, \theta)\hat{r}^a + \tau_2(r, \theta)\hat{\theta}^a \\ g\Phi^a &= \Phi_1(r, \theta)\hat{r}^a + \Phi_2(r, \theta)\hat{\theta}^a \end{aligned} \quad (3.1)$$

The spatial spherical coordinate orthonormal unit vectors are

$$\begin{aligned} \hat{r}_i &= \sin\theta\cos\phi\delta_{i1} + \sin\theta\sin\phi\delta_{i2} + \cos\theta\delta_{i3} \\ \hat{\theta}_i &= \cos\theta\cos\phi\delta_{i1} + \cos\theta\sin\phi\delta_{i2} - \sin\theta\delta_{i3} \\ \hat{\phi}_i &= -\sin\phi\delta_{i1} + \cos\phi\delta_{i2} \end{aligned} \quad (3.2)$$

and the isospin coordinate orthonormal unit vectors are

$$\begin{aligned} \hat{r}^a &= \sin\theta\cos n\phi\delta_1^a + \sin\theta\sin n\phi\delta_2^a + \cos\theta\delta_3^a \\ \hat{\theta}^a &= \cos\theta\cos n\phi\delta_1^a + \cos\theta\sin n\phi\delta_2^a - \sin\theta\delta_3^a \\ \hat{\phi}^a &= -\sin n\phi\delta_1^a + \cos n\phi\delta_2^a \end{aligned} \quad (3.3)$$

The  $\phi$ -winding number,  $n$ , is a natural number corresponds to the topological charge of dyon soluton.

#### 3.2 The Higgs Field

The general Higgs fields in the spherical and rectangular coordinate systems are

$$\begin{aligned} g\Phi^a &= \Phi_1(x)\hat{r}^a + \Phi_2(x)\hat{\theta}^a + \Phi_3(x)\hat{\phi}^a \\ &= \tilde{\Phi}_1(x)\delta^{a1} + \tilde{\Phi}_2\delta^{a2} + \tilde{\Phi}_3\delta^{a3} \end{aligned} \quad (3.4)$$

respectively, where

$$\tilde{\Phi}_1 = \sin\theta\cos n\phi\Phi_1 + \cos\theta\cos n\phi\Phi_2 - \sin n\phi\Phi_3 = |\Phi|\sin\alpha\cos\beta$$

$$\begin{aligned}\tilde{\Phi}_2 &= \sin \theta \sin n\phi \Phi_1 + \cos \theta \sin n\phi \Phi_2 + \cos n\phi \Phi_3 = |\Phi| \sin \alpha \sin \beta \\ \tilde{\Phi}_3 &= \cos \theta \Phi_1 - \sin \theta \Phi_2 = |\Phi| \cos \alpha\end{aligned}\quad (3.5)$$

The axially symmetric Higgs unit vector in the rectangular coordinate system is given by

$$\begin{aligned}\hat{\Phi}^a &= \sin \alpha \cos \gamma \delta^{a1} + \sin \alpha \sin \gamma \delta^{a2} + \cos \alpha \delta^{a3} \\ \cos \alpha &= h_1(r, \theta) \cos \theta - h_2(r, \theta) \sin \theta, \quad \sin \alpha = h_1(r, \theta) \sin \theta + h_2(r, \theta) \cos \theta \\ h_1(r, \theta) &= \frac{\Phi_1}{|\Phi|}, \quad h_2(r, \theta) = \frac{\Phi_2}{|\Phi|}, \quad \gamma = n\phi\end{aligned}\quad (3.6)$$

### 3.3 The Magnetic and Electric Fields

Following the definition of  $\cos \alpha$  (3.6), we can rewrite the Higgs part of the 't Hooft magnetic field (2.6) in a different form

$$gB_i^H = -n\epsilon_{ijk}\partial^j \cos \alpha \partial^k \phi \quad (3.7)$$

The gauge part of the magnetic field can similarly be rewritten as

$$gB_i^G = -n\epsilon_{ijk}\partial^j \cos \kappa \partial^k \phi \quad (3.8)$$

where  $\cos \kappa = P_1 h_2 - P_2 h_1$ . Hence the sum of the Higgs part (3.7) and gauge part (3.8) gives a different definition of 't Hooft magnetic field

$$gB_i = -n\epsilon_{ijk}\partial_j (\cos \alpha + \cos \kappa) \partial_k \phi = -n\epsilon_{ijk}\partial_j \mathcal{A}_k \quad (3.9)$$

where  $\mathcal{A}_i$  is the 't Hooft gauge potential. The magnetic field lines of the half dyon system can be pictured by representing the contour lines of  $(\cos \alpha + \cos \kappa) = \text{constant}$  on the vertical plane  $\phi = 0$ .

For the electric charge, the Abelian electric field is

$$\mathcal{E}_i = F_{i0} = \partial_i A_0 = \partial_i \{\tau_1 \cos(\alpha - \theta) + \tau_2 \sin(\alpha - \theta)\} = \partial_i |\tau| \quad (3.10)$$

where  $|\tau| = \sqrt{\tau_1^2 + \tau_2^2}$ , since the time component of the gauge field  $A_0^a$  is parallel to the Higgs field  $\hat{\Phi}^a$  in isospin space. In contrast to the magnetic field, the electric field changes in proportion to the electric charge parameter, which is between 0 and 1. By setting  $\eta = 0$ , it is possible to turn off the electric field. We can calculate the total electric charge  $Q$  of the system by numerically evaluating the volume integration and consider the case of axially symmetric dyon

$$Q = \int_V \partial^i \mathcal{E}_i d^3x = 2\pi \iint \partial^i \mathcal{E}_i r^2 \sin \theta dr d\theta \quad (3.11)$$

At spatial infinity in the Higgs vacuum, the non-Abelian components of the gauge potential become zero, and the non-Abelian electromagnetic field approaches a particular value, which is given by

$$\begin{aligned}F_{\mu\nu}^a|_{r \rightarrow \infty} &= [\partial_\mu A_\nu - \partial_\nu A_\mu - \frac{1}{g} \epsilon^{bcd} \hat{\Phi}^b \partial_\mu \hat{\Phi}^c \partial_\nu \hat{\Phi}^d] \hat{\Phi}^a \\ &= F_{\mu\nu} \hat{\Phi}^a\end{aligned}\quad (3.12)$$

where  $F_{\mu\nu}$  is the 't Hooft electromagnetic field. However, Coleman [15] argues that there is no single unique way to represent the Abelian electromagnetic field in the area surrounding the monopole outside the Higgs vacuum at finite values of  $r$ . One approach, proposed by 't Hooft, as in Eq. (2.5), results in a magnetic field with the unique feature that the magnetic charge density vanishes when  $|\Phi| \neq 0$ , whereas  $\partial^i B_i \neq 0$  when  $|\Phi| = 0$ , and the magnetic charges are located at these points. Consequently, with 't Hooft's definition of the electromagnetic field, the magnetic charges are individual and located at the point zeros of the Higgs field, resulting in a discrete magnetic charge at a specific point, and there is no magnetic charge distribution throughout the space. Another proposal for the Abelian electromagnetic field was presented by Bogomol'nyi [3] and Faddeev [16], in which the magnetic and electric fields are less singular and given respectively

$$\mathcal{B}_i = B_i^a \left( \frac{\Phi^a}{\nu} \right), \quad \mathcal{E}_i = E_i^a \left( \frac{\Phi^a}{\nu} \right) \quad (3.13)$$

respectively, where  $\nu$  is the vacuum expectation value of the Higgs field. With this definition, we can obtain the electromagnetic field in a less singular form and be able to visualize both electric and magnetic charge distributions in finite  $r$  region produced by the non-Abelian components of the gauge field. At spatial infinity in Higgs vacuum, both definitions of the electromagnetic field (2.5) and (3.13) become identical. To obtain the 3D surface graph of magnetic charge density, we will instead plot using the weighted magnetic charge density which is defined as  $M_d = (\partial^i \mathcal{B}_i) r^2 \sin \theta$  because the nature of magnetic charge density of half dyon solution is singular yet integrable. Similar technique will be used when plotting the weighted electric charge density,  $E_d = (\partial^i \mathcal{E}_i) r^2 \sin \theta$ .

### 3.4 The Magnetic Dipole Moment

From Maxwell's electromagnetic theory, the 't Hooft gauge potential,  $\mathcal{A}_i$ , Eq. (3.9) at large  $r$  tends to

$$\mathcal{A}_i = (\cos \alpha + \cos \kappa) \partial_i \phi \Big|_{r \rightarrow \infty} = \frac{\hat{\phi}_i}{r \sin \theta} \left\{ \frac{n}{2} (\cos \theta + 1) + \frac{F_G(\theta)}{r} \right\} \quad (3.14)$$

$$F_G(\theta) = \mu_m \sin^2 \theta + \nu_m \left\{ \sin^2 \theta \ln \left| \frac{1 + \cos \theta}{\sin \theta} \right| + \cos \theta \right\} \quad (3.15)$$

where  $\mu_m$  is the dimensionless magnetic dipole moment of the half monopole. We can calculate  $F_G(\theta)$  from numerical solution with the following expression

$$F_G(\theta) = nr \left[ (-P_2 + \cos \theta) h_1 + (P_1 - \sin \theta) h_2 - \frac{1}{2} (\cos \theta + 1) \right] \Big|_{r \rightarrow \infty} \quad (3.16)$$

We can obtain the value of magnetic dipole moment of the half monopole by plotting  $F_G(\theta)$  versus angle  $\theta$ . The constant  $\nu_m$  is, nonetheless, zero and we have  $F_G(\theta) = \mu_m \sin^2 \theta$ . The value of  $\mu_m$  can then be read directly from the graph of  $F_G(\theta)$  versus  $\theta$  at  $\theta = \pi/2$ .

### 3.5 The Energy

The total energy of the system is

$$E = \int_V \varepsilon d^3x \quad (3.17)$$

where  $\varepsilon$  is the energy density of the SU(2) Yang-Mills-Higgs theory given by

$$\varepsilon = B_i^a B_i^a + E_i^a E_i^a + D_i \Phi^a D_i \Phi^a + D_0 \Phi^a D_0 \Phi^a + \frac{\lambda}{2} (\Phi^a \Phi^a - \nu^2)^2 \quad (3.18)$$

By dimensionless transformations, we can change  $\varepsilon$  to a dimensionless value  $\tilde{\varepsilon}$ . Consider the case with axial symmetry, we have

$$E = 2\pi \iint \varepsilon r^2 \sin \theta dr d\theta = \frac{2\pi\nu}{g} \iint \tilde{\varepsilon} x^2 \sin \theta dx d\theta \quad (3.19)$$

Hence the total energy of the system  $E$  is in unit of  $2\pi\nu/g$ .

### 3.6 The Boundary Conditions and Numerical Calculations

The numerical half dyon solution is solved by substituting the Ansatz (3.1) into the equations of motion (2.3) which resulted in eight coupled nonlinear second order partial differential equations. At large distances ( $r \rightarrow \infty$ ), the half dyon solution is given by [11]

$$\begin{aligned} \psi_1 &= \frac{1}{2}, & P_1 &= \sin \theta - \frac{1}{2}(1 + \cos \theta) \sin\left(\frac{\theta}{2}\right) \\ R_1 &= 0, & P_2 &= \cos \theta - \frac{1}{2}(1 + \cos \theta) \cos\left(\frac{\theta}{2}\right) \\ \Phi_1 &= \cos\left(\frac{\theta}{2}\right), & \Phi_2 &= -\sin\left(\frac{\theta}{2}\right) \\ \tau_1 &= \eta \cos\left(\frac{\theta}{2}\right), & \tau_2 &= -\eta \sin\left(\frac{\theta}{2}\right) \end{aligned} \quad (3.20)$$

In this region, it is obvious that  $\Phi_1 \propto \tau_1$  and  $\Phi_2 \propto \tau_2$  that is the time component of gauge field and the Higgs field are parallel in the isospin space. We have the trivial vacuum solution close to the origin ( $r = 0$ ). The asymptotic solution and boundary conditions at  $r = 0$  which will produce finite energy half dyon solution are

$$\begin{aligned} \psi_1(0, \theta) &= P_1(0, \theta) = R_1(0, \theta) = P_2(0, \theta) = 0 \\ \sin \theta \Phi_1(0, \theta) + \cos \theta \Phi_2(0, \theta) &= 0 \\ \sin \theta \tau_1(0, \theta) + \cos \theta \tau_2(0, \theta) &= 0 \\ \frac{\partial}{\partial r} \{ \cos \theta \Phi_1(r, \theta) - \sin \theta \Phi_2(r, \theta) \} \Big|_{r=0} &= 0 \\ \frac{\partial}{\partial r} \{ \cos \theta \tau_1(r, \theta) - \sin \theta \tau_2(r, \theta) \} \Big|_{r=0} &= 0 \end{aligned} \quad (3.21)$$

The boundary conditions will be imposed on the profile functions along the positive  $z$ -axis ( $\theta = 0$ ) as follows:

$$\partial_\theta \psi_1 = P_1 = R_1 = P_2 = \partial_\theta \Phi_1 = \Phi_2 = \partial_\theta \tau_1 = \tau_2 = 0 \quad (3.22)$$

The boundary conditions imposed along the negative  $z$ -axis ( $\theta = \pi$ ) are

$$\partial_\theta \psi_1 = P_1 = R_1 = \partial_\theta P_2 = \Phi_1 = \partial_\theta \Phi_2 = \tau_1 = \partial_\theta \tau_2 = 0 \quad (3.23)$$

To perform numerical calculations, we transform the spatial coordinates  $r$  into dimensionless coordinates  $x$  using the relationship  $x = g\nu r$ , and rescale the profile functions by factors of  $\nu$  and  $g\nu$ :  $\Phi_1 \rightarrow \nu\Phi_1$ ,  $\Phi_2 \rightarrow \nu\Phi_2$ ,  $\tau_1 \rightarrow g\nu\tau_1$ , and  $\tau_2 \rightarrow g\nu\tau_2$ . This process results in a system of equations that depends solely on  $n$ ,  $\eta$ , and  $\beta$ , where  $\beta^2 = \lambda/g^2$ . Furthermore, it eliminates any dependence on the original variables  $g$ ,  $\nu$ , and  $\lambda$ . We discretize the system of equations using finite difference approximation on a non-equidistant grid of size  $70 \times 60$ . The grid covers the integration regions of  $0 \leq \tilde{x} \leq 1$  and  $0 \leq \theta \leq \pi$ , where  $\tilde{x} = x/(x+1)$  is the compactified coordinate. The derivatives with respect to  $x$  are then replaced with  $\tilde{x}$  using the relations,  $\partial_x \rightarrow (1-\tilde{x})^2\partial_{\tilde{x}}$  and  $\partial_{xx} \rightarrow (1-\tilde{x})^4\partial_{\tilde{x}\tilde{x}} - 2(1-\tilde{x})^3\partial_{\tilde{x}}$ . We solve the equations of motion Eq. 2.3 for  $\phi$ -winding number,  $1 \leq n \leq 4$ , the electric charge parameter,  $0 \leq \eta < 1$ , and with the Higgs self-coupling constant,  $\beta = 0.7782$ . The error arises from our numerical results is  $\mathcal{O}(10^{-3})$ .

## 4 Results

By implementing the appropriate boundary conditions, Eqs. (3.20) to (3.23), we have computed numerical solutions for the profile functions  $\psi_1$ ,  $R_1$ ,  $P_1$ ,  $P_2$ ,  $\tau_1$ ,  $\tau_2$ ,  $\Phi_1$ , and  $\Phi_2$  for  $\phi$ -winding numbers,  $n$ , ranging from 0 to 4 and for electric charge parameters,  $\eta$ , ranging from 0 to 1. It is important to note that no solutions were found for  $n$  values greater than 4. When  $n = 4$ , a critical electric charge parameter of 0.9354 exists. The presence of electric charge is directly related to the value of  $\eta$ , which means that we have the standard half monopole solutions when  $\eta = 0$ , and dyon solutions can be obtained when  $\eta$  is greater than zero.

Next, we calculate and graph the modulus of the Higgs field,  $|\Phi|$ , the weighted energy density,  $\epsilon_d$ , the weighted magnetic charge density,  $M_d$ , and the weighted electric charge density,  $E_d$ , numerically for the  $x-z$  plane at  $y = 0$ . The general shape of the dyons resembles the findings of Teh et al. [11], which is a balloon-like shape that expands from the origin and extends along the negative  $z$ -axis. As  $n$  and  $\eta$  increase, the half-dyon's size stretches along the negative  $z$ -axis, but its shape remains unchanged.

From the graphs of Higgs modulus, we observe that the inverted cone shape stretches further down the negative  $z$ -axis as  $\eta$  increases, and the zeros of Higgs modulus also increase along the negative  $z$ -axis. Similarly, the length of the Higgs modulus along the negative  $z$ -axis also increases, but at a greater rate as  $n$  increases than with increases in  $\eta$ . Fig. 1 illustrates the 3D and contour plots of the Higgs modulus,  $|\Phi|$ . The peak value of the weighted energy density,  $\epsilon_d$ , is 15.15 at  $z = -4.916$  ( $n = 2$ ,  $\eta = 0.9$ ) and 22.09 at  $z = -8.849$  ( $n = 4$ ,  $\eta = 0.9$ ). The energy is integrable along the negative  $z$ -axis, and from Fig. 1 e), f), and g), it has no singularities, indicating that the half dyon solutions possess finite energy.

Fig. 2 depicts the plots of the weighted electric charge density,  $E_d$ , of the half dyon system. As  $n$  and  $\eta$  increase, the peak of the electric charge density extends along the negative  $z$ -axis from the origin. This observation is supported by the contour plots, which indicate that the increase is only limited to the negative  $z$ -direction. Additionally, we observe that the total electric charge,  $Q$ , of the system is increasing, as the magnitude of the electric charge density also increases with an increase in  $n$ .

The behavior of the weighted magnetic charge density,  $M_d$ , is similar to that of the weighted electric charge density, as the size only changes along the negative  $z$ -axis when  $n$  and  $\eta$  increase. From Fig. 3, we observe that while an increase in  $\eta$  does not significantly affect the magnetic field strength, it elongates the magnetic charge distribution along the negative  $z$ -axis. This observation

Table 1: Selected values for electric charge per  $n$ ,  $Q/n$ , in unit of  $2\pi/g$ , magnetic dipole moment per  $n$ ,  $\mu_m/n$ , in unit of  $1/g$  and energy per  $n$ ,  $E/n$  in unit of  $2\pi\nu/g$  with Higgs self-coupling constant  $\beta = 0.7782$  for  $\phi$ -winding number  $1 \leq n \leq 4$ .

$n = 1$										
$\eta$	0	0.2	0.3	0.4	0.5	0.6	0.7	0.8	0.9	0.99
$Q/n$	0	0.1671	0.2552	0.3495	0.4529	0.5695	0.7057	0.8706	1.0790	1.3117
$\mu_m/n$	0.6879	0.6974	0.7097	0.7280	0.7534	0.7878	0.8339	0.8960	0.9809	1.0873
$E/n$	2.7519	2.7661	2.7855	2.8157	2.8606	2.9266	3.0241	3.1711	3.4013	3.7394
$n = 2$										
$\eta$	0	0.2	0.3	0.4	0.5	0.6	0.7	0.8	0.9	0.99
$Q/n$	0	0.1633	0.2488	0.3392	0.4367	0.5442	0.6652	0.8039	0.9653	1.1199
$\mu_m/n$	1.3103	1.3256	1.3452	1.3740	1.4131	1.4644	1.5307	1.6153	1.7228	1.8453
$E/n$	2.9120	2.9261	2.9449	2.9739	3.0159	3.0755	3.1592	3.2773	3.4465	3.6652
$n = 3$										
$\eta$	0	0.2	0.3	0.4	0.5	0.6	0.7	0.8	0.9	0.99
$Q/n$	0	0.1648	0.2503	0.3390	0.4317	0.5305	0.6413	0.7700	0.9147	1.0564
$\mu_m/n$	1.9252	1.9452	1.9701	2.0046	2.0489	2.1073	2.1920	2.2969	2.3982	2.5252
$E/n$	3.0189	3.0335	3.0524	3.0805	3.1194	3.1717	3.2432	3.3521	3.5121	3.7119
$n = 4$										
$\eta$	0	0.2	0.3	0.4	0.5	0.6	0.7	0.8	0.9	0.9354
$Q/n$	0	0.1756	0.2641	0.3530	0.4423	0.5323	0.6236	0.7172	0.8164	0.8662
$\mu_m/n$	2.5252	2.6559	2.6763	2.6961	2.7165	2.7385	2.7643	2.7981	2.8559	2.9242
$E/n$	3.0911	3.0978	3.1187	3.1524	3.1988	3.2586	3.3327	3.4230	3.5347	3.5886

is supported by the corresponding contour plots. Fig. 3 also outlines the magnetic field lines of the half dyon configuration. As  $\eta$  increases, the magnetic charge extends gradually towards the negative  $z$ -axis, and this extension increases significantly with an increase in  $n$ . Thus, we can conclude that the half dyon system has both magnetic and electric charge densities that extend towards the negative  $z$ -axis from the origin.

The numerical values of the total electric charge per  $n$ ,  $Q/n$ , magnetic dipole moment per  $n$ ,  $\mu_m/n$ , and total energy per  $n$ ,  $E/n$ , for the half dyon system are computed and presented in Table 1. Additionally, the graphs in Fig. 4 illustrate the relationship between these values and  $\eta$ . The graphs indicate that the total electric charge per  $n$  decreases with increasing  $n$ , while both the energy per  $n$ ,  $E/n$ , and the magnetic dipole moment per  $n$ ,  $\mu_m/n$ , increase as  $n$  increases. We also calculate the magnetic charge of the system with half dyon using Eq. (2.7), we find  $2\pi/g$ ,  $4\pi/g$ ,  $6\pi/g$  and  $8\pi/g$  for  $n = 1, 2, 3$  and  $4$  respectively. Therefore, confirm numerically that its net magnetic charge is  $2n\pi/g$ . Furthermore, the total energy of the half dyon configuration in unit of  $2\pi\nu/g$  for  $n = 1, 2, 3$ , and  $4$  at  $\eta = 0.9$  are 3.4013, 6.8930, 10.5363, and 14.1388, respectively.

## 5 Comments

In summary, our analysis shows that the half dyon solutions tend to be located near the origin, with a semi-infinite string extending along the negative  $z$ -axis. As the  $\phi$ -winding number increases, the length of the half dyons extends further along the negative  $z$ -axis, and multiple half dyons become superimposed near the origin. We find that these solutions possess finite energy, indicating their stability in the theory. We also confirm numerically that the net magnetic charge of our half dyon configuration is  $2n\pi/g$  for integer  $n$  up to 4.

## References

- [1] P.A.M. Dirac, Proc. R. Soc. London A 133 (1931) 60.
- [2] G. 't Hooft, Nucl. Phys. **B79** (1974) 276; A.M. Polyakov, Sov. Phys. - JETP **41** (1975) 988; Phys. Lett. **B59** (1975) 82; JETP Lett. **20** (1974) 194.
- [3] E.B. Bogomol'nyi and M.S. Marinov, Sov. J. Nucl. Phys. **23** (1976) 357.
- [4] M.K. Prasad and C.M. Sommerfield, Phys. Rev. Lett. **35** (1975) 760; E.B. Bogomol'nyi, Sov. J. Nucl. Phys. **24** (1976) 449.
- [5] C. Rebbi and P. Rossi, Phys. Rev. **D22** (1980) 2010; R.S. Ward, Commun. Math. Phys. **79** (1981) 317; P. Forgacs, Z. Horvarth and L. Palla, Phys. Lett. **99** (1981) 232; Nucl. Phys. **B192** (1981) 141; M.K. Prasad, Commun. Math. Phys. **80** (1981) 137; M.K. Prasad and P. Rossi, Phys. Rev. **D24** (1981) 2182.
- [6] E.J. Weinberg and A.H. Guth, Phys. Rev. **D14** (1976) 1660.
- [7] Rosy Teh and K.M. Wong, J. Math. Phys. **46**, (2005) 082301; Int. J. Mod. Phys. A 20,(2005) 4291.
- [8] P.M. Sutcliffe, Int. J. Mod. Phys. **A12** (1997) 4663; C.J. Houghton, N.S. Manton and P.M. Sutcliffe, Nucl.Phys. **B510** (1998) 507.
- [9] B. Kleihaus and J. Kunz, Phys. Rev. **D61** (2000) 025003; B. Kleihaus, J. Kunz, and Y. Shnir, Phys. Lett. **B570** (2003) 237; B. Kleihaus, J. Kunz, and Y. Shnir, Phys. Rev. **D68** (2003) 101701; Phys. Rev. **D70** (2004) 065010.
- [10] E. Harikumar, I. Mitra, and H.S. Sharatchandra, Phys. Lett. **B557** (2003) 303.
- [11] R. Teh, B.L. Ng and K.M. Wong, Mod. Phys. Lett. A **27** (2012) 1250233; J. Phys. G: Nucl. Part. Phys. **40** (2013) 035004.
- [12] E. Witten, Phys. Lett. **B86**, 283 (1979).
- [13] B. Julia and A. Zee, Phys. Rev. **D11**, 2227 (1975); F.A. Bais and J.R. Primack, Phys. Rev. **D13**, 819 (1976).
- [14] S. Coleman, S.Parke, A. Neveu, and C.M. Sommerfield, Phys. Rev. **D15**, 544 (1977).

- [15] S. Coleman, *New Phenomena in Subnuclear Physics (International School of Subnuclear Physics 'Ettore Majorana)* ed A. Zichichi (New York: Plenum, 1975) p 297.
- [16] L. D. Faddeev, *Nonlocal, nonlinear and nonrenormalisable field theories Proc. 4th Int. Symp. on Nonlocal Field Theories* (Joint Institute for Nuclear Research, Alushta, Dubna, 1976) p 207; L.D. Faddeev, *Lett. Math. Phys.* **1** (1976) 289.

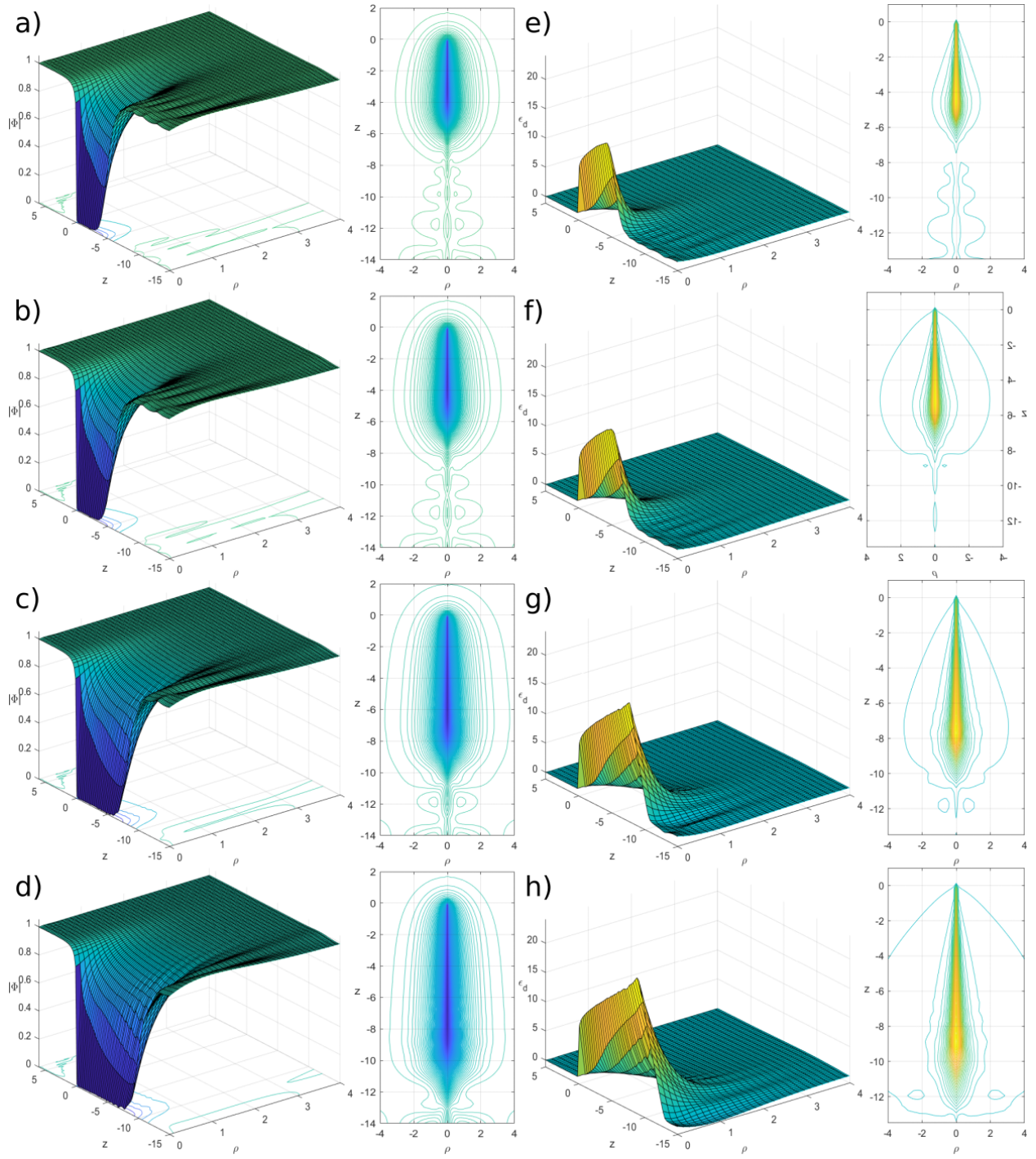


Figure 1: Higgs modulus and its contour of the half dyon for a)  $n = 2, \eta = 0.6$  b)  $n = 2, \eta = 0.9$  c)  $n = 3, \eta = 0.9$  d)  $n = 4, \eta = 0.9$ . Weighted energy density and its contour of the half dyon for e)  $n = 2, \eta = 0.6$  f)  $n = 2, \eta = 0.9$  g)  $n = 3, \eta = 0.9$  h)  $n = 4, \eta = 0.9$

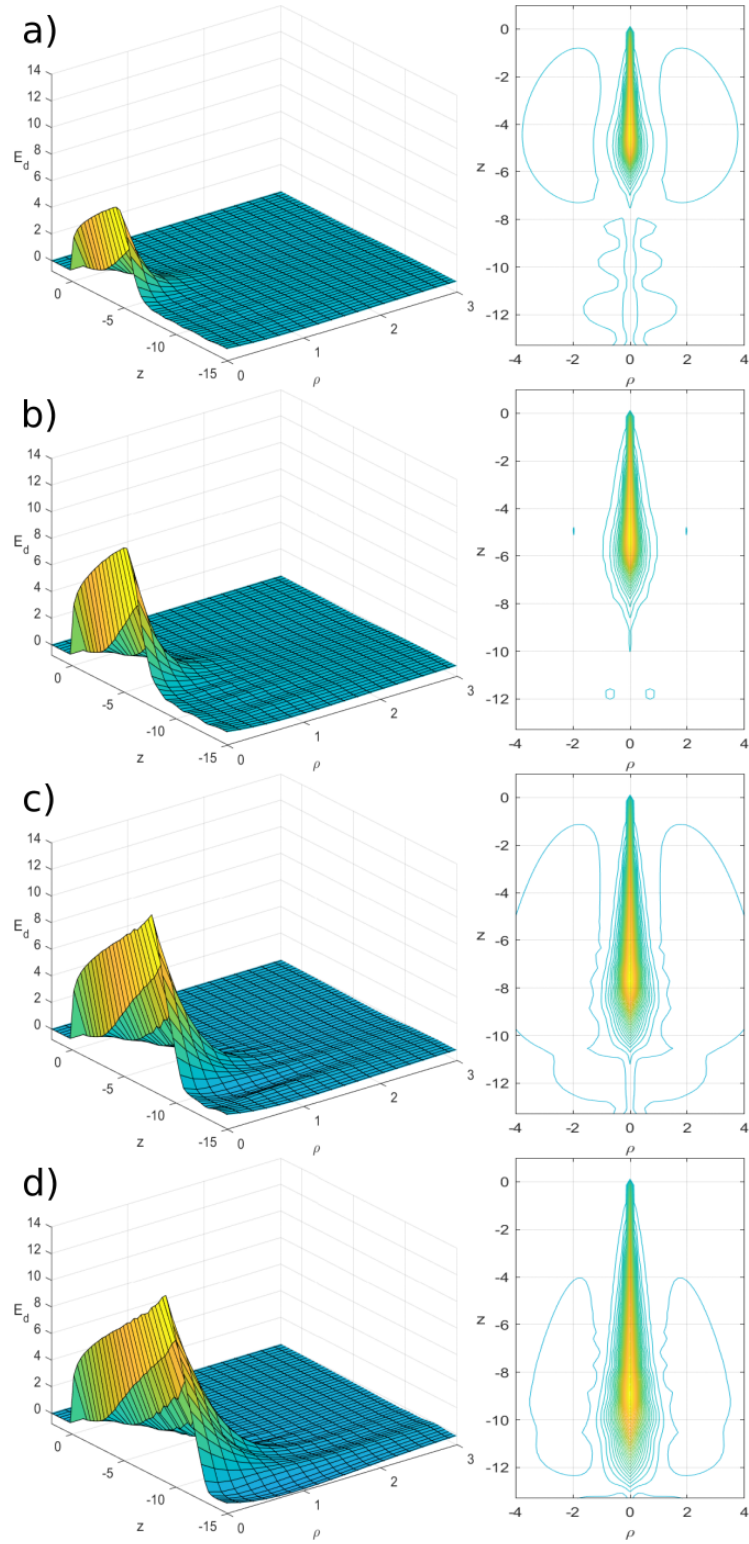


Figure 2: Weighted electric density and its contour of the half dyon for a)  $n = 2, \eta = 0.6$  b)  $n = 2, \eta = 0.9$  c)  $n = 3, \eta = 0.9$  d)  $n = 4, \eta = 0.9$

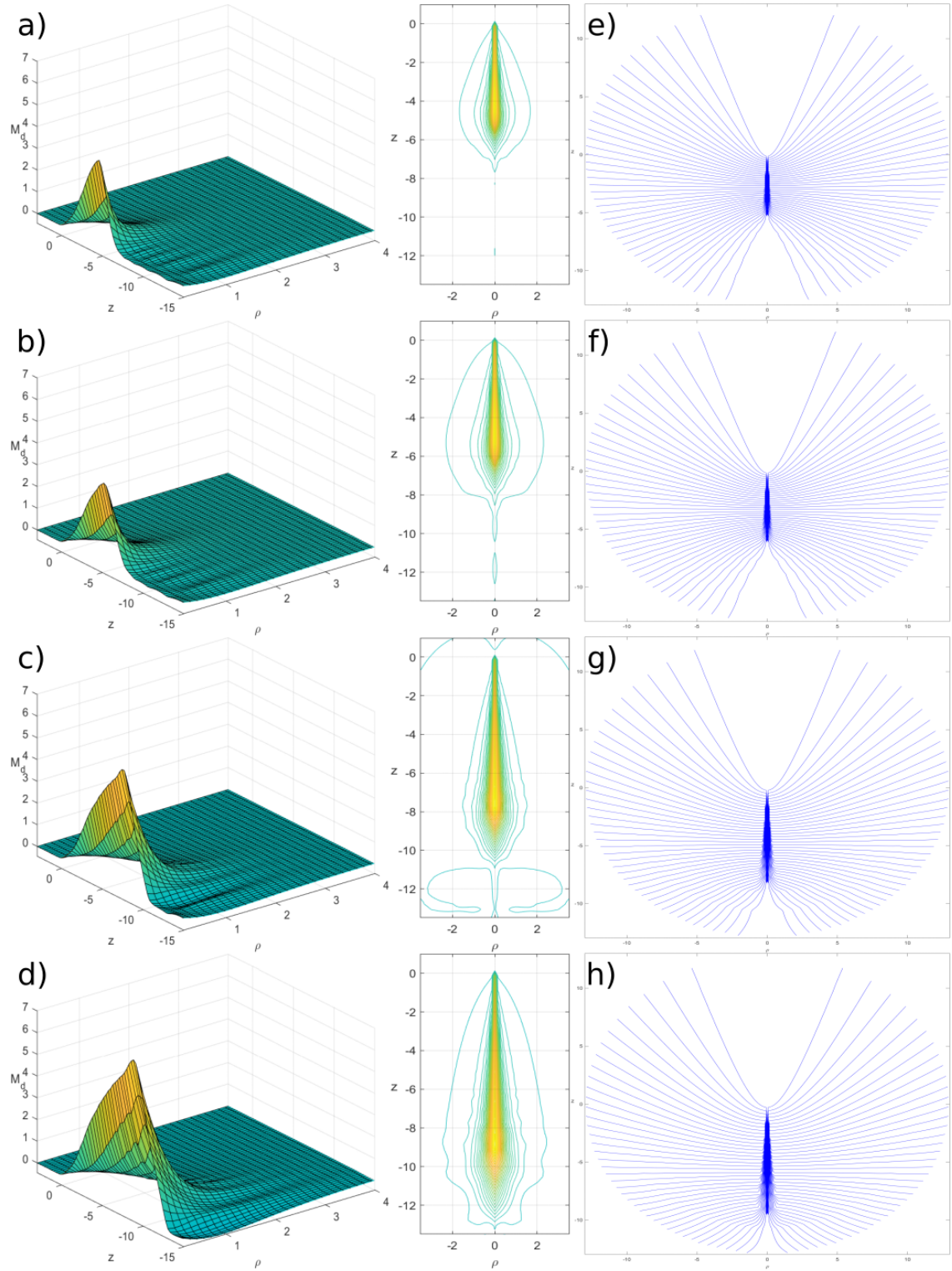


Figure 3: Weighted magnetic density and its contour of the half dyon for a)  $n = 2, \eta = 0.6$  b)  $n = 2, \eta = 0.9$  c)  $n = 3, \eta = 0.9$  d)  $n = 4, \eta = 0.9$ . Magnetic field lines of the half dyon for e)  $n = 2, \eta = 0.6$  f)  $n = 2, \eta = 0.9$  g)  $n = 3, \eta = 0.9$  h)  $n = 4, \eta = 0.9$

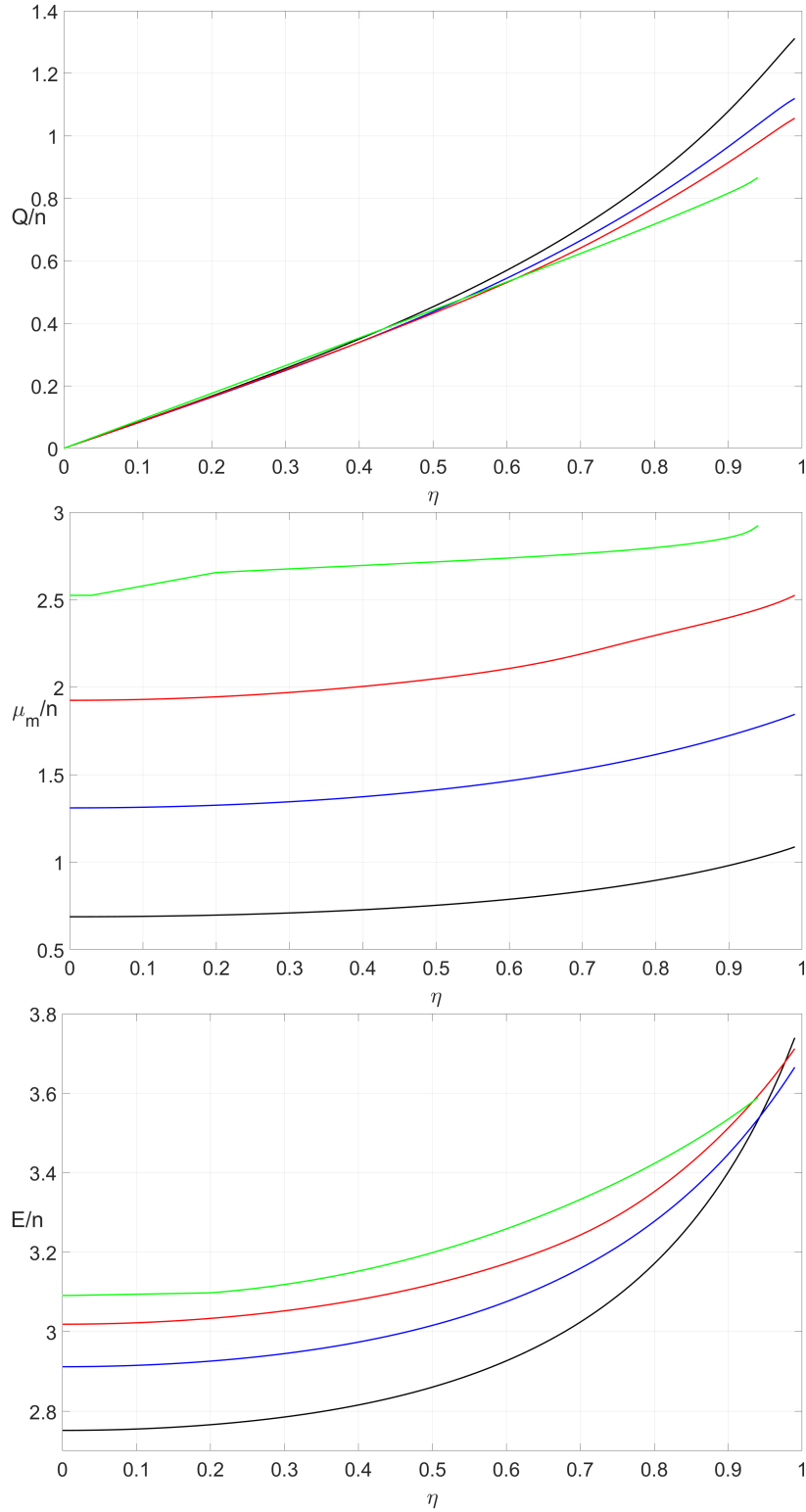


Figure 4: Plots of a)  $Q/n$  versus  $\eta$ , b)  $\mu_m/n$  versus  $\eta$  c)  $E/n$  versus  $\eta$  of the half dyon solutions for  $n = 1$  (black),  $n = 2$  (blue),  $n = 3$  (red) and  $n = 4$  (green).